

The Effect of Interatomic Potentials on the Molecular Dynamics Simulation of Nanometric Machining

Akinjide Oluwajobi Xun Chen

Centre for Precision Technologies, University of Huddersfield, Queensgate, Huddersfield HD1 3DH, UK

Abstract: One of the major tasks in a molecular dynamics (MD) simulation is the selection of adequate potential functions, from which forces are derived. If the potentials do not model the behaviour of the atoms correctly, the results produced from the simulation would be useless. Three popular potentials, namely, Lennard-Jones (LJ), Morse, and embedded-atom method (EAM) potentials, were employed to model copper workpiece and diamond tool in nanometric machining. From the simulation results and further analysis, the EAM potential was found to be the most suitable of the three potentials. This is because it best describes the metallic bonding of the copper atoms; it demonstrated the lowest cutting force variation, and the potential energy is most stable for the EAM.

Keywords: Interatomic potentials, molecular dynamics (MD), nanomachining, modelling, material removal.

1 Introduction

Metal removal technologies play essential roles in modern manufacturing^[1, 2]. The demand for miniaturized devices with very high dimensional accuracy and surface finish is making ultra-precision processes the major choices in mechanical, optical, medical and electronic applications. Currently, it is very difficult to study the various mechanisms of material removal in nanometric machining through experiments. Also, at this length scale, analytical and empirical models are limited by measurement problems^[3].

Conventionally, the tool-workpiece interface has been considered to be homogeneous and subsequently analyzed using continuum mechanics. In nanomachining, the interface often contains a few atoms or layers of atoms, which should be based on discrete atomistic analysis.

The molecular dynamics (MD) simulation technique has been applied effectively in the investigation and prediction of machining processes at the nanoscale. This method can improve our understanding of nanometric processes and subsequently give helpful insights into phenomena that are otherwise intractable to investigate experimentally^[4, 5].

The MD method was first used in the study of statistical mechanics in the late 1950s, by Alder and Wainwright^[6]. Since then, the simulation method has been applied in materials science, mechanical engineering and other disciplines. The major task in an MD simulation is the selection of an adequate interatomic potential function, and if the potential does not model the behaviour of the atoms correctly, the results produced from the simulation would be useless.

Belak and Stowers^[7] pioneered work on the study of cutting copper with a diamond tool. At first, the method was used extensively to illustrate nano-cutting processes (see Fig. 1). In 1991, Belak and Stowers^[8] applied the MD to abrasive processes and Rentsch and Inasaki^[9] later presented the results of simulations on the pile-up phenomenon in abrasive machining.

Unlike in conventional cutting processes, where the undeformed chip thickness is significant compared to the cutting edge radius, in nanomachining, the undeformed chip thickness is very small. Therefore, the cutting edge effects cannot

be ignored. The effect of tool geometry in nanometric cutting was investigated by Komanduri et al.^[10] MD studies were conducted with various tool edge radii (1.81–21.72 nm) and depths of cut (0.362–2.172 nm) at constant ratios (0.1, 0.2, and 0.3) of the depth of cut to the tool edge radius (d/R). Results showed that with tools of different radii, the cutting force increase with depth of cut, independent of the (d/R) ratio^[10].

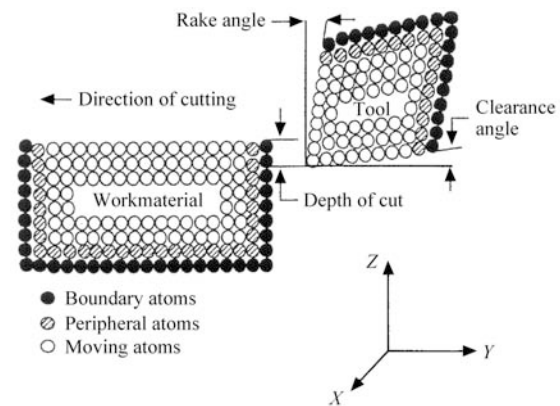


Fig. 1 The MD simulation of nanometric cutting (2D)^[11]

The MD method has been used in a variety of application areas, namely, indentation^[12, 13], wear and friction^[14, 15], void growth^[16, 17], etc.

Notations.

a_i	: Acceleration of atom i .
d	: Depth of cut.
D	: Material dependent constant.
E	: Energy of interacting particles.
E_{tot}	: Total embedding energy.
F_i	: Force acting on atom i .
F_x, F_y, F_z	: Tangential, lateral and normal components of the cutting forces respectively (eV/Angs = 1.602×10^{-9} N).
G_i	: Embedding energy for placing atom i into the electron density.
h	: Planck constant (6.626069×10^{-34} J.s).
\hbar	: Reduced Planck constant
	$\frac{h}{2\pi}$ (1.054571×10^{-34} ms ² kg/s).
k_B	: Boltzmann constant

	$(1.3806504 \times 10^{-23} \text{ JK}^{-1})$.
m	: Mass of interacting particles.
m_i	: Mass of atom or particle i .
N	: Number of atoms.
r	: Distance between atoms.
R	: Tool edge radius.
r_e	: Equilibrium distance between atoms i and j .
r_i	: Position of atom or particle i .
r_{ij}	: Instantaneous distance between particles i and j .
r_n	: Position of the n -th atom or particle.
t	: Time.
T_{current}	: Current temperature that is calculated from the kinetic energy.
T_{desired}	: Desired temperature.
T_i	: Temperature of the i -th atom.
v	: Velocity.
v_i	: Velocity of atom i .
$v_{i,\text{new}}$: Newly scaled velocity of atom i .
$V_1, V_2, V_3, \dots, V_m$: m -body potentials.
$V, V_{ij}, V(r_{ij})$: Interatomic pair potential (short range pair interaction representing the core-core repulsion).
$Z_{ij}, Z(r_{ij})$: Effective charge function.
α	: Material dependent constant.
ε	: Material dependent constant.
σ	: Material dependent constant.
$\rho_{h,i}$: Total electron density at atom i due to the rest of the atoms in the system.
$\Psi(r, t)$: Wave function (the probability of finding any particle at position r , at time t).

2 Fundamentals of MD and examples of MD simulations of nanomachining

MD is a computer simulation technique by which the atomic trajectories of a system of N particles are generated by the numerical integration of Newton's equation of motion^[18]. It is a deterministic method, which implies that the state of the system at any future time can be predicted from its current state^[19]. The method is also based on statistical mechanics — a probabilistic approach used to obtain a set of configurations distributed according to some statistical ensemble^[20].

The MD simulation consists of the numerical step-by-step solution of the classical equations of motion based on Newton's second law. For a set of N particles or atoms,

$$F_i = m_i a_i \quad (1)$$

where m_i is the mass of atom i , $a_i = \frac{d^2 r_i}{dt^2}$, the acceleration of the atom i and F_i is the force acting on atom i . (The forces are usually obtained as the gradient of a potential energy function).

Rentsch and Inasaki^[9] modelled a copper workpiece and a diamond tool using the Lennard-Jones (LJ) potential function for the copper atom interactions. They assumed the boundaries and the tool to be rigid; and observed a pronounced build-up phenomenon after 25 000 time steps.

Komanduri et al.^[21] used a copper workpiece and an infinitely hard tungsten tool for their simulation. They used Morse potentials and a cutting speed of 500 m/s. Ye et al.^[22] investigated the chemical-mechanical polishing of copper by a single abrasive particle, using the embedded-

atom method (EAM) potential. Lin et al.^[23] studied the features of grinding energy dissipation, grinding stress, strain state, grinding temperature; the nanoscale material removal mechanism and surface generation. They used silicon as both the workpiece and the tool material; and applied the Tersoff potential function for the simulation. Brinksmeier et al.^[24] obtained a three-dimensional MD simulation of the grinding process using the EAM potential. They modelled two abrasives that cut through a workpiece of 100 000 atoms over its whole length at 100 m/s.

Pei et al.^[25] and Promyoo et al.^[26] carried out MD simulations of the nanometric cutting of copper with diamond tool. They both studied the effects of the tool rake angle and the interatomic potentials (Morse and EAM) on the process. Pei et al.^[25] found out that there is no big difference in the simulated chip formation, but Morse potential results in about 5–70 % higher cutting forces than the EAM potential. They both found EAM to be better than Morse potential for the simulations. Their studies were based on two-dimensional models, but the performance of three-dimensional simulations remains unknown.

3 Interatomic potentials for MD

The energy of N interacting particles can be written as^[27, 28]

$$E = \sum_i V_1(r_i) + \sum_{i < j} V_2(r_i r_j) + \sum_{i < j < k} V_3(r_i r_j r_k) + \dots \quad (2)$$

where r_n is the position of the n -th particle and the functions V_1, V_2, V_3, \dots are the m -body potentials.

The second term in (2) is the two-body or the pair potential and the third term is the three-body potential. Other higher terms are neglected because it is believed that the right-hand side of the equation have a quick convergence and they are difficult to handle in calculations^[29].

Therefore, it follows that the potential of a system $V(r_1, r_2, \dots, r_N)$ can be assumed to be the sum of the effective pair potentials $V(r_{ij})$ as,

$$V = \sum_i \sum_{j > i} V(r_{ij}) \quad (3)$$

where r_{ij} is the distance between particles i and j .

The LJ pair potential is the most commonly used interaction model^[20]. Morse is also an example of a pair potential, which is suitable for modelling cubic metals. The EAM is a many-body potential, which is used for a wider range of metals.

3.1 Lennard-Jones (LJ) potential^[30]

$$V_{ij} = 4\varepsilon \left[\left(\frac{\sigma}{r} \right)^{12} - \left(\frac{\sigma}{r} \right)^6 \right] \quad (4)$$

where ε and σ are constants that are dependent on the physical property of the materials.

3.2 Morse potential^[31]

$$V_{ij} = D \{ \exp[-2\alpha(r_{ij} - r_e)] - 2 \exp[-\alpha(r_{ij} - r_e)] \} \quad (5)$$

where r_{ij} and r_e are instantaneous and equilibrium distances between atoms i and j , respectively, α and D are constants determined on the basis of the physical properties of the material.

3.3 Embedded-atom potential (EAM)^[32, 33]

$$E_{\text{tot}} = \sum_i G_i(\rho_{h,i}) + \frac{1}{2} \sum_{i,j} V_{ij}(r_{ij}) \quad (6)$$

where $\rho_{h,i}$ is the total electron density at atom i because of the rest of the atoms in the system; G_i is the embedding energy for placing an atom into the electron density; V_{ij} is the short range pair interaction representing the core-core repulsion; r_{ij} is the separation of atoms i and j .

4 Simulation

Table 1 shows the simulation conditions applied in this research. The workpiece consists of 16 000 copper atoms with perfect face-centred cubic (FCC) lattice. It includes 3 kinds of atoms, namely, boundary atoms, thermostat atoms, and Newtonian atoms. The boundary atoms are kept fixed to reduce edge effects. The thermostat atoms conduct the heat generated during the cutting process out of the cutting region. This is achieved by the velocity scaling of the thermostat atoms with the conversion between the kinetic energy (KE) and temperature via (7)^[34, 35].

$$\sum_i \frac{1}{2} m_i v_i^2 = \frac{3}{2} N k_B T_i \quad (7)$$

where m_i is the mass of the i -th atom, v_i is the resultant velocity of the i -th atom, N is the number of the thermostat atoms, T_i is the temperature of the i -th atom and k_B is the Boltzmann constant ($1.3806504 \times 10^{-23} \text{ J} \cdot \text{K}^{-1}$).

Table 1 MD simulation parameters

Parameters	Values
Bulk temperature	293 K
Cutting direction	[100]- Along the x -axis
Cutting speed	150 m/s
Cutting depth	1.0 nm
Time step	0.3 fs
Run	100 000 steps

Whenever the temperature of the thermostat atoms exceeds the preset bulk temperature of 293 K, their velocities are scaled by using (8)^[36, 37].

$$v_{i,\text{new}} = v_i \sqrt{\frac{T_{\text{desired}}}{T_{\text{current}}}} \quad (8)$$

where T_{current} is the current temperature that is calculated from the KE, and T_{desired} is the desired temperature.

The Newtonian atoms obey Newton's equation of motion. The cutting tool consists of 912 carbon atoms with diamond lattice structure. The cutting tool is pointed shaped and it is modelled as a rigid body.

Fig. 2 shows the MD simulation model.

The atomic interactions in the simulation are the following:

- Cu-Cu: Interactions between copper atoms.
- Cu-C : Interactions between copper atoms and diamond atoms.
- C-C : Interactions between the diamond atoms (treated as rigid in this paper)

The LAMMPS MD software^[38] was used for the simulations and the VMD software^[39] was used for the visualization of the results.

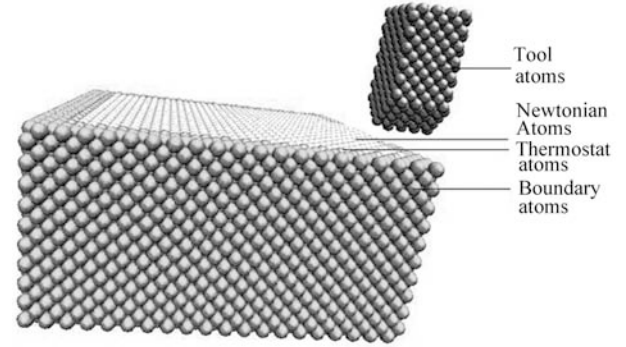


Fig. 2 The MD simulation model

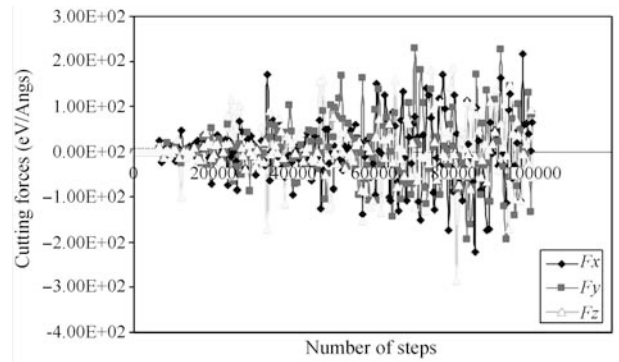
4.1 Modelling with LJ potential

Equation (4) is used, where σ and ε are constants, which are dependent on the physical property of the material. The LJ parameters used for the atom interactions are $\sigma = 2.2277 \text{ Angstroms}$ and $\varepsilon = 0.415 \text{ eV}$ ^[40], which apply to both the Cu-Cu and the Cu-C interactions.

The simulation and the cutting forces are shown in Fig. 3 (a) and (b). The potential energy and the total energy for the LJ modelling are given in Fig. 4 and the temperature variation is shown in Fig. 5.



(a) Simulation with LJ potential



(b) Cutting forces for LJ potential

Fig. 3 Simulation and cutting forces for LJ potential

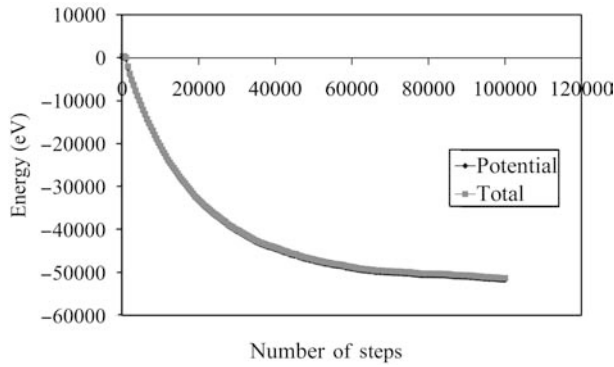


Fig. 4 Potential and total energies for LJ potential

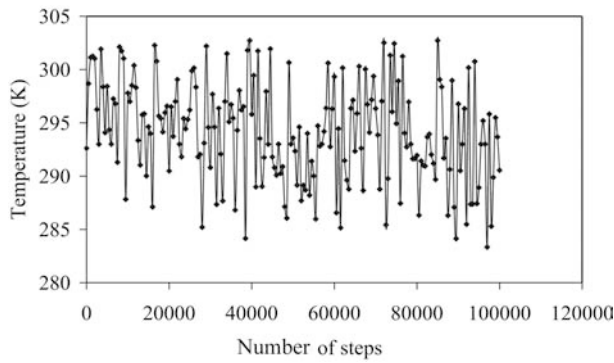


Fig. 5 Temperature variation for LJ potential

4.2 Modelling with morse potential

Equation (5) is used:

1) For Cu-Cu interactions^[25, 41]:

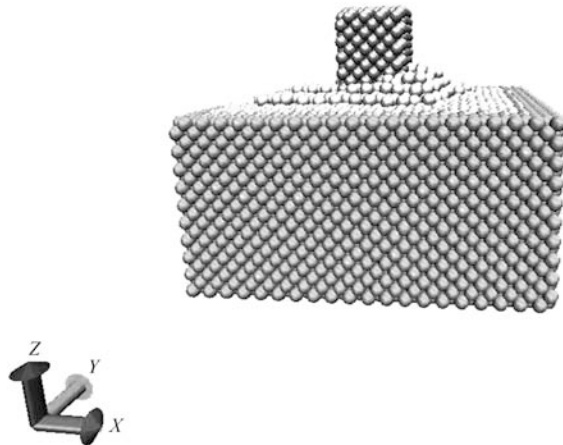
$$D = 0.3429 \text{ eV}, \quad \alpha = 0.13588 (\text{nm})^{-1}, \quad r_e = 0.2866 \text{ nm}.$$

2) For Cu-C interactions^[40]:

$$D = 0.087 \text{ eV}, \quad \alpha = 0.17 (\text{nm})^{-1}, \quad r_e = 0.22 \text{ nm}.$$

The cut-off distance was 6.4 Angstroms (that is, the interactions between atoms separated by more than this distance are neglected).

The simulation and the cutting forces are shown in Fig. 6 (a) and (b). The potential energy and the total energy for the Morse modelling are given in Fig. 7 and the temperature variation is shown in Fig. 8.



(a) Simulation with Morse potential

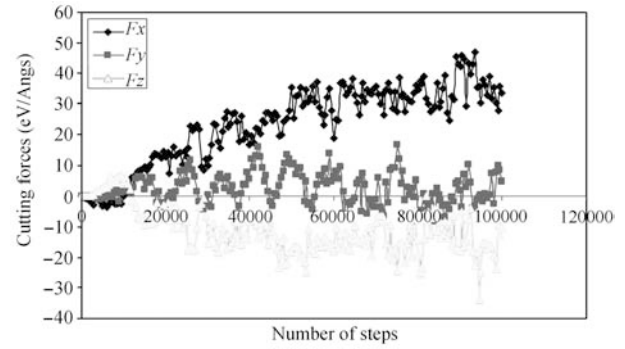
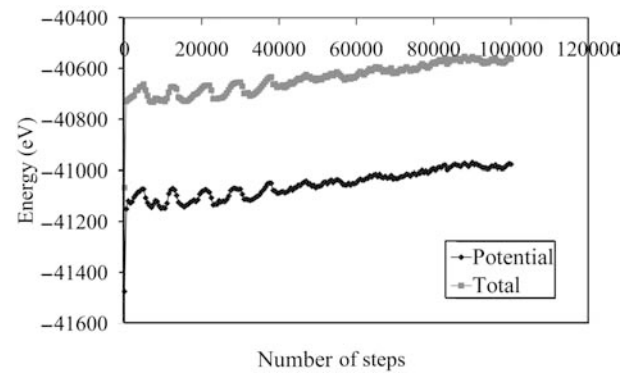
(b) Cutting forces for Morse potential
Fig. 6 Simulation and cutting forces for Morse potential

Fig. 7 Potential and total energies for Morse potential

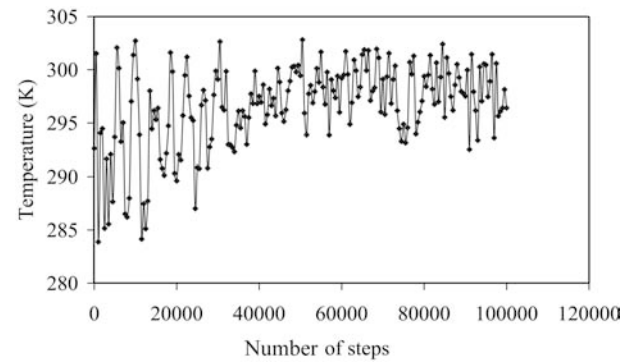


Fig. 8 Temperature variation for Morse potential

4.3 Modelling with EAM potential

Equation (6) is used, where the potential parameters used for the Cu-Cu interactions were read from the file Cu_u3.eam in LAMMPS. The file contains the following: the lattice constant of copper (3.615 Angstroms), the spacing in density (5.01E-4) and the spacing in distance (1.00E-2). Also, it contains three arrays of tabulated values of the embedding function, $G_i(\rho_{h,i})$ —500 values; effective charge function, Z_{ij} —500 values, from which the pair potential interaction is calculated (the relationship between the effective charge and the pair potential is given by (9)) and the density function, $\rho_{h,i}$ —500 values (a total of 1 500 tabulated values). The cut-off distance was 4.95 Angstroms^[40].

(There are no available EAM potential parameters between Cu and C atoms^[25]).

$$V_{ij}(r_{ij}) = \frac{Z^2(r_{ij})}{r_{ij}}. \quad (9)$$

For a more realistic situation, another simulation (see Fig. 9) was also carried out with EAM potentials for the Cu-Cu interactions (with parameters same as above) and Morse potential parameters for the Cu-C interactions. The Morse parameters used are below^[40]:

$$D = 0.087 \text{ eV}, \quad \alpha = 0.17 \text{ (nm)}^{-1}, \quad r_e = 0.22 \text{ nm}.$$

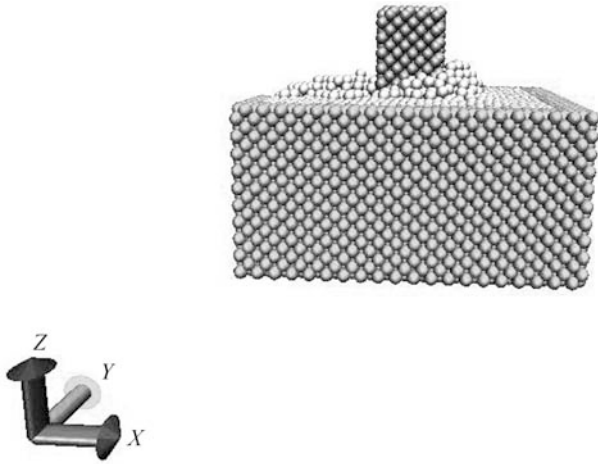


Fig. 9 Simulation with EAM-Morse potentials

The comparison of potential energy in the two simulations (EAM and the EAM-Morse) shows that the error or difference is very minimal (see Fig. 10). Because the forces are derived from the potential energy, the difference in the cutting forces will also be small.

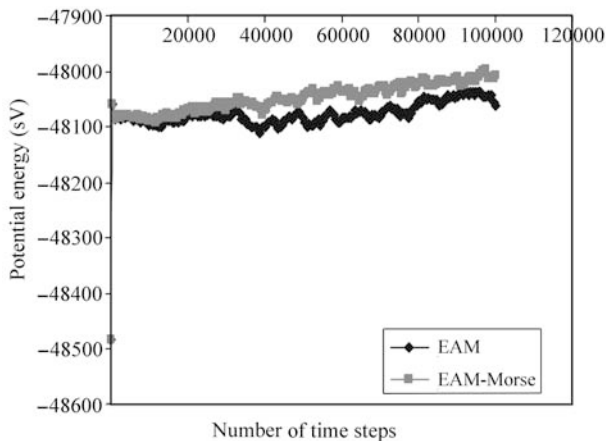
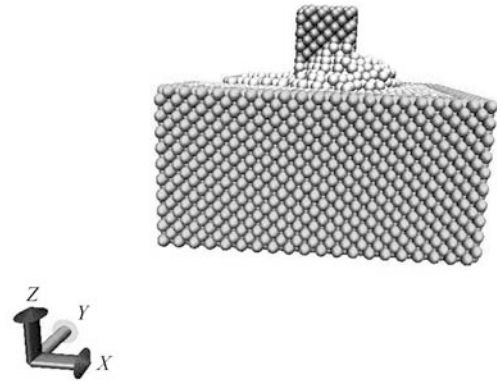
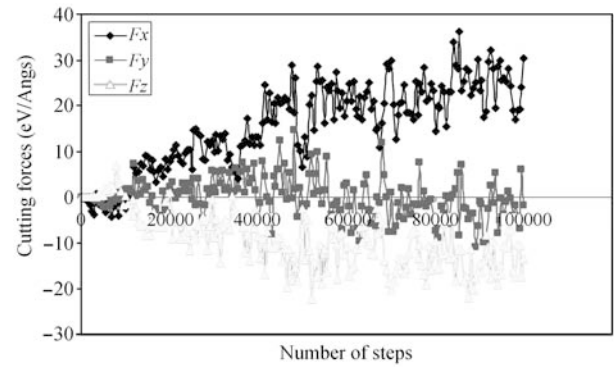


Fig. 10 The comparison of the potential energy for the EAM and the EAM-Morse potentials

The simulation and the cutting forces for the EAM modelling are shown in Fig. 11 (a) and (b). The potential energy and the total energy are given in Fig. 12, and the temperature variation is shown in Fig. 13.



(a) Simulation with EAM potential



(b) Cutting forces for EAM potential

Fig. 11 Simulation and cutting forces for EAM potential

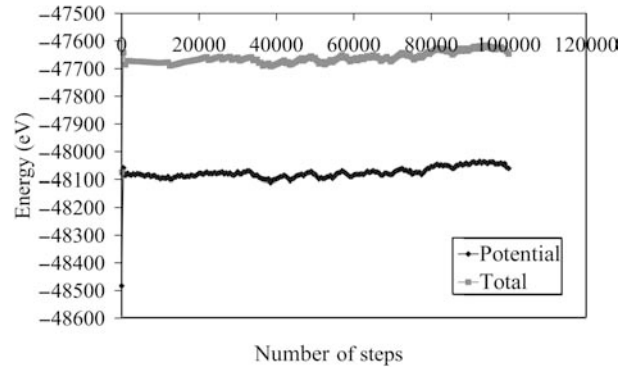


Fig. 12 Potential and total energies for EAM potential

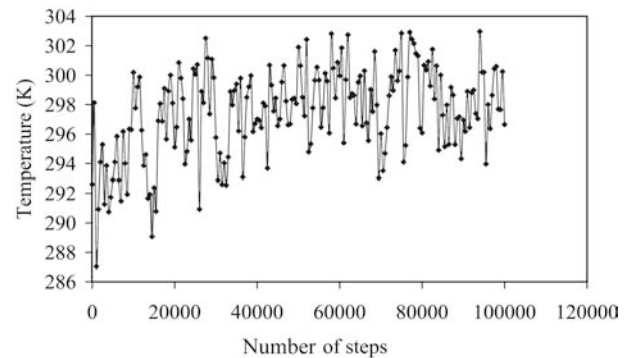


Fig. 13 Temperature variation for EAM potential

5 Results and discussion

For the LJ model, the potential energy and total energy were initially unstable, but stabilized after 60 000 steps. Also, the potential energy was initially high but reduced considerably to around -5200 eV , towards the end of the simulation at 100 000 steps (see Figs. 4 and 14); the tangential component of cutting forces varied in the range from around -354E-9 N to 346E-9 N with an average of -1.33E-9 N ($\text{eV}/\text{\AA} = 1.602 \times 10^{-9} \text{ N}$); the phenomenon of ploughing was not observed. As observed in Fig. 3 (a), the copper atoms behave more like gases rather than solids, as they do not show the cohesiveness in solids — they loosely move around. The temperature variation shows a slight average decrease with the increase in the number of simulation steps. For the Morse model, the potential energy and total energy fluctuate initially and stabilize after 80 000 steps. Also, the potential is higher than for the EAM potential (see Fig. 14); the tangential component of cutting forces are in the range from around -5.62E-9 N to 70.51E-9 N with an average of 37.34E-9 N ; the phenomenon of ploughing was observed with pile-up of 4 layers of atoms. The temperature variation shows a slight average increase with the increase in the number of simulation steps. The atoms behave as in solids — bonded together. For the EAM model, the potential energy and total energy were relatively stable. Also, the potential energy is lower compared with the Morse potential; the tangential component of cutting forces are in the range from around -6.74E-9 N to 58.2E-9 N with an average of 24.99E-9 N ; the phenomenon of ploughing was observed, with pile-up of 5 layers of atoms. The temperature variation shows a slight average increase with the increase in the number of simulation steps. The atoms behave as in solids — bonded together, similar to what was observed for the Morse potential. The ratio between the tangential, lateral and the normal components of the cutting forces is similar to that found in conventional machining for the Morse and the EAM potentials. The results of the EAM model are comparable with those in [25, 26], where the EAM potential best describes the metallic bonding in the copper atoms. In contrast, the pair potentials (both LJ and Morse potentials), do not incorporate the many-body effects; they have no environmental dependence and they do not account for the directional nature of bonding in metals^[29].

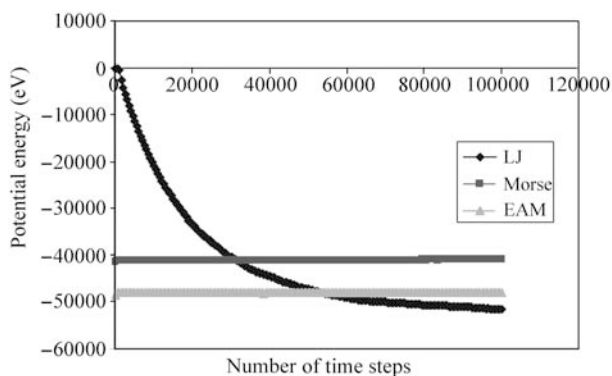


Fig. 14 The variation of potential energies for the LJ, Morse, and EAM potentials

6 Conclusions

Through this investigation, it is identified that the EAM potential is the most appropriate of the 3 potentials commonly used for the modelling of nanomachining of copper with diamond tool. This is because the EAM potential provides the best description of the metallic bonding in the workpiece. Also, the cutting forces variation is smallest; the potential and total energies are most stable for the depth of cut considered. Therefore, the EAM potential should be used, rather than LJ and Morse potentials for the modelling of copper and other FCC metals in MD simulations of nanomachining.

References

- [1] K. K. B. Hon, B. T. H. T. Buharudin. The impact of high speed machining on computing and automation. *International Journal of Automation and Computing*, vol. 3, no. 1, pp. 63–68, 2006.
- [2] X. Chen, T. Limchimchol. Monitoring grinding wheel redress-life using support vector machines. *International Journal of Automation and Computing*, vol. 3, no. 1, pp. 56–62, 2006.
- [3] R. Rentsch. Nanoscale cutting. *Nano and Micromachining*, J. P. Davim, M. J. Jackson, Eds., USA: Wiley-ISTE, pp. 1–24, 2008.
- [4] A. O. Oluwajobi, X. Chen. The effect of interatomic potentials on nanometric abrasive machining. In *Proceedings of the 16th International Conference on Automation and Computing*, Birmingham, UK, pp. 130–135, 2010.
- [5] A. O. Oluwajobi, X. Chen. The fundamentals of modelling abrasive machining using molecular dynamics. *International Journal of Abrasive Technology*, vol. 3, no. 4, pp. 354–381, 2010.
- [6] B. J. Alder, T. E. Wainwright. Studies in molecular dynamics. I. general method. *Journal of Chemical Physics*, vol. 31, no. 2, pp. 459–466, 1959.
- [7] J. F. Belak, I. F. Stowers. A molecular dynamics model of the orthogonal cutting process. In *Proceedings of the American Society of Precision Engineering*, ECD, New York, USA, pp. 76–79, 1999.
- [8] J. Belak, I. F. Stowers. The indentation and scratching of a metal surface: A molecular dynamics study. *Fundamentals of Friction: Macroscopic and Microscopic*, Pollock, Ed., USA: Singer, pp. 1–10, 1991.
- [9] R. Rentsch, I. Inasaki. Molecular dynamics simulation for abrasive processes. *Annals of the CIRP*, vol. 43, no. 1, pp. 327–330, 1994.
- [10] R. Komanduri, N. Chandrasekaran, L. M. Raff. Effect of tool geometry in nanometric cutting: A molecular dynamics simulation approach. *Wear*, vol. 219, no. 1, pp. 84–97, 1998.
- [11] R. Komanduri, L. M. Raff. A review on the molecular dynamics simulation of machining at the atomic scale. *Proceedings of the Institution of Mechanical Engineers, Part B: Journal of Engineering Manufacture*, vol. 215, no. 12, pp. 1639–1672, 2001.
- [12] S. D. Kenny, D. Mulliah, C. F. Sanz-Navarro, R. Smith. Molecular dynamics simulations of nanoindentation and nanotribology. *Philosophical Transactions of the Royal Society A*, vol. 363, no. 1833, pp. 1949–1959, 2005.
- [13] R. Smith, D. Christopher, S. Kenny. Defect generation and pileup of atoms during nanoindentation of Fe single crystals. *Physical Review B*, vol. 67, no. 24, pp. 1–10, 2003.
- [14] K. Cheng, X. Luo, R. Ward, R. Holt. Modeling and simulation of the tool wear in nanometric cutting. *Wear*, vol. 255, no. 7–12, pp. 1427–1432, 2003.

- [15] J. Shimizu, H. Eda, M. Yoritune, E. Ohmura. Molecular dynamics simulations of friction on the atomic scale. *Nanotechnology*, vol. 9, no. 2, pp. 118–123, 1998.
- [16] G. P. Potirniche, M. F. Horstemeyer, G. J. Wagner, P. M. Gullett. A molecular dynamics study of void growth and coalescence in single crystal nickel. *International Journal of Plasticity*, vol. 22, no. 2, pp. 257–278, 2006.
- [17] K. J. Zhao, C. Q. Chen, Y. P. Shen, T. J. Lu. Molecular dynamics study on the nano-void growth in face-centered cubic single crystal copper. *Computational Materials Science*, vol. 46, no. 3, pp. 749–754, 2009.
- [18] J. Li. Basic molecular dynamics. *Handbook of Materials Modelling*, S. Yip, Ed., Berlin, Germany: Springer, pp. 565–588, 2005.
- [19] A. Leach. *Molecular Modelling: Principles and Applications*, New Jersey, USA: Prentice Hall, 2001.
- [20] F. Ercolessi. *A Molecular Dynamics Primer*, [Online], Available: <http://www.fisica.uniud.it/~ercolessi/md/md/>, March 5, 2011.
- [21] R. Komanduri, N. Chandrasekaran, L. M. Raff. Some aspects of machining with negative-rake tools simulating grinding: A molecular dynamics simulation approach. *Philosophical Magazine Part B*, vol. 79, no. 7, pp. 955–968, 1999.
- [22] Y. Ye, R. Biswas, J. R. Morris, A. Bastawros, A. Chandra. Simulation of nanoscale polishing of copper with molecular dynamics. In *Proceedings of Materials Research Society Symposium*, vol. 732E, pp. 1–6, 2002.
- [23] B. Lin, S. Y. Yu, S. X. Wang. An experimental study on molecular dynamics simulation in nanometer grinding. *Journal of Materials Processing Technology*, vol. 138, no. 1–3, pp. 484–488, 2003.
- [24] E. Brinksmeier, J. C. Aurich, E. Govekar, C. Heinzel, H. W. Hoffmeister, F. Klocke, J. Peters, R. Rentsch, D. J. Stephenson, E. Uhlmann, K. Weinert, M. Wittmann. Advances in modeling and simulation of grinding processes. *Annals of the CIRP*, vol. 55, no. 2, pp. 667–696, 2006.
- [25] Q. X. Pei, C. Lu, F. Z. Fang, H. Wu. Nanometric cutting of copper: A molecular dynamics study. *Computational Materials Science*, vol. 37, no. 4, pp. 434–441, 2006.
- [26] R. Promyoo, H. E. Mounayri, X. Yang. Molecular dynamics simulation of nanometric machining under realistic cutting conditions. In *Proceedings of ASME International Conference on Manufacturing Science and Engineering*, Evanston, IL, USA, pp. 235–243, 2008.
- [27] J. Tersoff. New empirical approach for the structure and energy of covalent systems. *Physical Review B*, vol. 37, no. 12, pp. 6991–7000, 1988.
- [28] J. Tersoff. Empirical interatomic potential for silicon with improved elastic properties. *Physical Review B*, vol. 38, no. 14, pp. 9902–9905, 1988.
- [29] J. H. Li, X. D. Dai, S. H. Liang, K. P. Tai, Y. Kong, B. X. Lin. Interatomic potentials of the binary transition metal systems and some applications in materials physics. *Physics Reports*, vol. 455, no. 1–3, pp. 1–134, 2008.
- [30] J. E. Lennard-Jones. On the forces between atoms and ions. *Proceedings of the Royal Society of London*, vol. 109, no. 752, pp. 584–597, 1924.
- [31] P. M. Morse. Diatomic molecules according to the wave mechanics II vibrational levels. *Physical Review*, vol. 34, no. 1, pp. 57–64, 1929.
- [32] S. M. Foiles. Application of the embedded atom method to liquid transition metals. *Physical Review B*, vol. 32, no. 6, pp. 3409–3415, 1985.
- [33] S. M. Foiles, M. I. Baskes, M. S. Daw. Embedded-atom-method functions for the FCC metals Cu, Ag, Au, Ni, Pd, Pt, and their alloys. *Physical Review B*, vol. 33, no. 12, pp. 7983–7991, 1986.
- [34] M. Cai, X. Li, M. Rahman. Molecular dynamics modelling and simulation of nanoscale ductile cutting of silicon. *International Journal of Computer Applications in Technology*, vol. 28, no. 1, pp. 2–8, 2007.
- [35] Y. Guo, Y. Liang, M. Chen, Q. Bai, L. Lu. Molecular dynamics simulations of thermal effects in nanometric cutting process. *Science China Technological Sciences*, vol. 53, no. 3, pp. 870–874, 2010.
- [36] W. C. D. Cheong, L. Zhang, H. Tanaka. Some essentials of simulating nano-surface processes using the molecular dynamics method. *Key Engineering Materials*, vol. 196, pp. 31–42, 2001.
- [37] Z. Lin, Z. Chen, J. Huang. Establishment of a cutting force model and study of the stress-strain distribution in nano-scale copper material orthogonal cutting. *The International Journal of Advanced Manufacturing Technology*, vol. 33, no. 5–6, pp. 425–435, 2007.
- [38] S. J. Plimpton. Fast parallel algorithms for short-range molecular dynamics. *Journal of Computational Physics*, vol. 117, pp. 1–19, 1995.
- [39] Visual Molecular Dynamics (VMD), [Online], Available: <http://www.ks.uiuc.edu/Research/vmd/>, March 5, 2011.
- [40] H. J. Hwang, O. K. Kwon, J. W. Kang. Copper nanocluster diffusion in carbon nanotube. *Solid State Communications*, vol. 129, no. 11, pp. 687–690, 2004.
- [41] L. A. Girifalco, V. G. Weizer. Application of the morse potential function to cubic metals. *Physical Review*, vol. 114, no. 3, pp. 687–690, 1959.
- [42] LAMMPS Manual, [Online], Available: <http://lammps.sandia.gov/doc/>, March 5, 2011.



Akinjide Oluwajobi received the B.Sc. degree in engineering physics from Obafemi Awolowo University, Nigeria, M.Sc. degree in mechanical engineering from University of Ibadan, Nigeria, the MBA (production and operations management) from Obafemi Awolowo University, and the M.Sc. degree in complex systems from University of Pavia, Italy. He is currently a Ph.D. candidate at the Centre for Precision Technologies, School of Computing and Engineering, University of Huddersfield, UK, where he specialises in ultra precision engineering and nanotechnology. He has been a lecturer in mechanical engineering at Obafemi Awolowo University for over ten years.

His research interests include ultra precision engineering and nanotechnology, CAD/CAM, modelling and simulation of engineering systems, emerging technologies viz, fuzzy logic, neural networks, and evolutionary algorithms.

E-mail: j.o.oluwajobi@hud.ac.uk (Corresponding author)



Xun Chen received the B.Eng. degree from Fuzhou University. He received the M.Sc. degree from Zhejiang University, PRC, and the Ph.D. degree from Liverpool John Moores University. He was a visiting professor at Fuzhou University from 2001 to 2008. He is a reader in precision engineering at the University of Huddersfield, UK. He specialises in advanced manufacturing technology particularly in the high efficiency precision grinding. He is a founding member of the International Committee of Abrasive Technology. Before his employment at Huddersfield, he was an academician at the University of Nottingham, UK, the University of Dundee, UK, and Fuzhou University, PRC, and a research fellow, a Royal Society Royal Fellow at Liverpool John Moores University, UK.

His research interests include advanced manufacturing technology, advanced abrasive machining technology, intelligent process monitoring and control, knowledge support systems, and design for manufacturing (fixturing).

E-mail: x.chen@hud.ac.uk